



HAL
open science

Study of a foam flotation process assisted by cationic surfactant for the separation of soil clay particles: processing parameters and scaling-up sensitivity

Anouar Ben Said, Fabien Frances, Agnès Grandjean, Christelle Latrille,
Sylvain Faure

► To cite this version:

Anouar Ben Said, Fabien Frances, Agnès Grandjean, Christelle Latrille, Sylvain Faure. Study of a foam flotation process assisted by cationic surfactant for the separation of soil clay particles: processing parameters and scaling-up sensitivity. 2019. cea-04125705

HAL Id: cea-04125705

<https://cea.hal.science/cea-04125705>

Preprint submitted on 12 Jun 2023

HAL is a multi-disciplinary open access archive for the deposit and dissemination of scientific research documents, whether they are published or not. The documents may come from teaching and research institutions in France or abroad, or from public or private research centers.

L'archive ouverte pluridisciplinaire **HAL**, est destinée au dépôt et à la diffusion de documents scientifiques de niveau recherche, publiés ou non, émanant des établissements d'enseignement et de recherche français ou étrangers, des laboratoires publics ou privés.

**Study of a foam flotation process assisted by cationic surfactant for the
separation of soil clay particles: processing parameters and scaling-up
sensitivity**

Anouar Ben Said^a, Fabien Frances^a, Agnès Grandjean^a, Christelle Latrille^b, Sylvain Faure^{a*}

^a *CEA, DEN, DE2D, SEAD, Laboratoire des Procédés Supercritiques et de Décontamination,
F-30207 Bagnols sur Cèze, France*

^b *CEA, DEN, DPC, SECR, Laboratoire de Mesure et de Modélisation de la Migration des
Radionucléides, F-91191 Gif sur Yvette Cedex, France*

***Corresponding author:** sylvain.faure@cea.fr

Tel.: +33 4 66 39 74 19

E-mail adress: sylvain.faure@cea.fr

Postal address: CEA Marcoule, DE2D/SEAD/LPSD, Bât. 51, BP 17171, F-30207 Bagnols-
sur-Cèze, France

Abstract

Continuous froth flotation process assisted by cationic surfactant was employed in this study, as cost-effective and environmentally friendly technology, to separate fine phyllosilicates particles of soil. A continuous flotation column was specifically designed for soil flotation. The effects of processing parameters, including collector concentration expressed as collector/soil ratio (0.1-0.4%), froth residence time (45-150 s), suspension concentration (50-125 g/L) and air flow rate (0.5-2.5 L/min), upon separation performance were investigated in order to define the operating conditions which led to the best performance. The ability of the process to separate fine phyllosilicates particles was investigated and scale-up studies were performed at pilot scale. Flotation results showed that fine particles separation (<100 μm) from soil is feasible: separation rates between 15% and 40% are reached with low concentration of surfactant. Granulometric studies showed peak densities around 3, 10 and 40 μm , attributed to phyllosilicates, phyllosilicate aggregates and quartz particles. The mineralogical composition of the extracted particles were identified and discussed. Finally, the results obtained both at lab and pilot scales emphasized good agreement which provides valuable evidence to support the technical viability of the soil flotation process for future exploitation at industrial scale.

Keywords: Foam flotation process; soil decontamination; separation; phyllosilicates; surfactant; scale-up

1. Introduction

Despite the numerous radioactive soil decontamination technologies such as, soil washing [1], magnetic separation [2], electrokinetic processing [3], phytoremediation methods [4], there is a need for environmentally friendly process operating in continuous mode that will

limit the production of secondary wastes and the use of large amounts of organic chemicals, and allow reducing the high volumes of contaminated soil. It was reported in previous studies that in contaminated soils, the contamination is strongly related to the soil particles size; the finer the particle the higher is the contamination [5, 6]. In 2012, JAEA (Japan Atomic Energy Agency) demonstrated that, in Fukushima radio-contaminated soils, 87% of contamination is fixed on phyllosilicate particles smaller than 75 μm [7]. In order to decontaminate soils, our strategy is to separate phyllosilicate particles retaining the contamination due to their strong cesium adsorption properties [8, 9]. To do this, we propose a froth flotation technology assisted by cationic surfactant. As a first approach, the strategy was to evaluate the process efficiency to remove preferably phyllosilicates from non-contaminated soil.

Froth flotation is a physicochemical separation process that separates hydrophobic particles from a mixture of hydrophobic and hydrophilic particles. This technology is one of the main industrial applications of ions (ionic flotation) and solid particles (particle flotation) separation and it has been applied in various technological fields [10-12]. It has initially been used in mineral processing [13,14] and adopted, in recent years, for the treatment of industrial waste water [15], the recycling of plastics [16] and the pulp and paper industry for deinking and recycling of waste paper [17,18]. Flotation has also been employed in bioengineering for bacteria separation [19].

The most important condition enabling a high efficiency of flotation process is surface hydrophobicity. In our application, phyllosilicates minerals are hydrophilic negatively charged particles, that is why a cationic surfactant was selected to perform a partial hydrophobization. The surfactant adsorption on the phyllosilicates enables both hydrophobization of particles surface and neutralization of their surface charge. In the whole, the process involves the following unit steps: (i) generation and dispersion of air bubbles in the suspension containing surfactant collector, (ii) collision of hydrophobic particles with air

bubbles, (iii) adhesion of hydrophobic particles to air bubbles and formation of particle-bubble aggregates, (iv) ascension of particle-bubble aggregates from the suspension to the three-phase froth [20].

Within the last years, few research activities on clay flotation using cationic surfactant have been published [21-24]. Goldenberg et al. [21] investigated the processes of attachment of clay particles to bubble surfaces and their transport through an artificial porous medium. These processes occurred with no addition of traditional collectors. In their works, Huang et al. [22] performed comparative studies on flotation of aluminosilicate minerals with Gemini quaternary ammonium salt surfactants (BDDA and EDDA). They compared the flotation behaviors of pure kaolinite, pyrophyllite and illite. They found that the three phyllosilicates exhibited good floatability with Gemini cationic surfactants as collectors over a wide pH range, while BDDA showed a stronger collecting power than EDDA. Jiang et al. [23] studied the flotation behaviors and adsorption mechanisms of quaternary ammonium cationic collectors (dodecyltrimethylammonium chloride, DTAC) and (cetyltrimethylammonium chloride, CTAC) on kaolinite. Xia et al. [24] employed Gemini quaternary ammonium salt surfactant and its corresponding conventional monomeric surfactant dedecyl trimethyl ammonium bromide (DTAB) for the flotation of illite, pyrophyllite and kaolinite. They made a comparative study between the floatabilities of these minerals using the different surfactants. These previous studies highlighted the necessity to add cationic surfactant to enhance the negatively charged phyllosilicate particles attachment on bubbles. **Although previous studies have used cationic surfactant to hydrophobize phyllosilicates, the first major innovative point of our study consists to apply particulate flotation process assisted by cationic surfactant to a complex mixture of particles such as a natural raw clay soil (real soil) in order to extract preferentially negatively charged phyllosilicates. The second major innovative point deals with the column flotation design. This study refers to the first**

continuous flotation column dedicated to separate phyllosilicates in soil. Its design permits to measure the separation rate as a function of foam height (residence time). Moreover ~~The innovation of this study is to specify~~ **specifies** the size of particles floated and separated from soil, and **identifies** their mineralogical composition. ~~To the best of our knowledge, our study is the first one aiming to the selective separation of fine phyllosilicate particles from soil by flotation technology.~~ Likewise, the present study will look at the influence of processing parameters on flotation efficiency and selectivity to **phyllosilicates** particles, and the investigation of the flotation process scalability. At first, this work aims at adapting the froth flotation process in a continuous operation mode to the separation of fine particles from soil and studying its performance: separation rate, size distribution and structure of the separated particles. Second, it aims at investigating the impact of the most significant process parameters, including collector amount, froth residence time, suspension concentration and air flow rate upon the separation rate, as well as identifying the process parameters that better affect the flotation. Finally, it aims at examining the process selectivity to fine particles and investigating its scalability.

2. Experimental approach

2.1. Materials

The soil used in this study was a loamy acidic soil (pH=5.5, measured in water). This non contaminated soil sample was collected closed to a French Nuclear Site at a depth between 0-14 cm. It was then sieved through a 2 mm mesh, dried in ambient air for one week and stirred to obtain homogenized samples for flotation trials. To maintain the original particle size, we did not remove any organic material from samples. Tetradecyltrimethylammonium bromide (TTAB) cationic surfactant was selected as collector, having a CMC of 3.6 mmol/L. It was supplied by Fluka with a purity higher than 98%. Flotation experiments described in this paper were carried out with soil suspensions prepared in Milli-Q® grade pure water (15

MΩ.cm at 25 °C). To do that, the desired soil amount was added into 40 L of pure water under stirring 500 round/min during 30 min in order to ensure efficient particles dispersion, then TTAB was added at the desired concentration, during mixing. Soil-TTAB suspensions were prepared 20 minutes before starting the flotation experiments.

2.2. Flotation process

2.2.1. Principles and basics

The principle of the flotation operation is schematically presented in Fig. 1. It consists of the capture by air bubbles of finely dispersed hydrophobic particles to produce the so-called "three-phase froth". Flotation exploits the differences in surface hydrophobicity of the different particles dispersed in a suspension and selectively separates the desired particles by attaching them to air bubbles and recover them in a laden froth. Hydrophobic particles are attached to the bubble surface due to hydrophobic interaction, whereas hydrophilic particles remain dispersed in the aqueous suspension [25, 26]. This process is mainly achieved by adding appropriate chemical reagent (collector) to enlarge the floatability difference between target particles (hydrophobic) and the other ones (hydrophilic) [24]. Therefore, the collector is one of the key factors in flotation separation; furthermore, it can be a cationic or an anionic surfactant.

In general, a typical way to improve flotation efficiency of fine and negatively charged particles (phyllosilicates in our case) is achieved by the addition of cationic surfactant. When a small amount of cationic surfactant is added, it acts at first hand as a foaming agent; it stabilizes bubbles surfaces through the reduction of interfacial tensions. On the other hand, it acts as collector; it causes the neutralization of particles surface charge, resulting in an aggregation of fine particles which improve the flotation. In our case, phyllosilicates are hydrophilic negatively charged particles and therefore they cannot directly attach to air

bubbles, which justifies the addition of cationic surfactant to perform their hydrophobization and to enhance their attachment to air bubbles.

2.2.2. Experimental set-up

Flotation experiments were conducted in a flotation column operating in continuous mode and able to handle suspensions having relatively high particle size (the particle diameter can reach 2.5 mm).

The flotation experimental set-up used in this study to perform flotation tests is schematically drawn on Fig. 1.

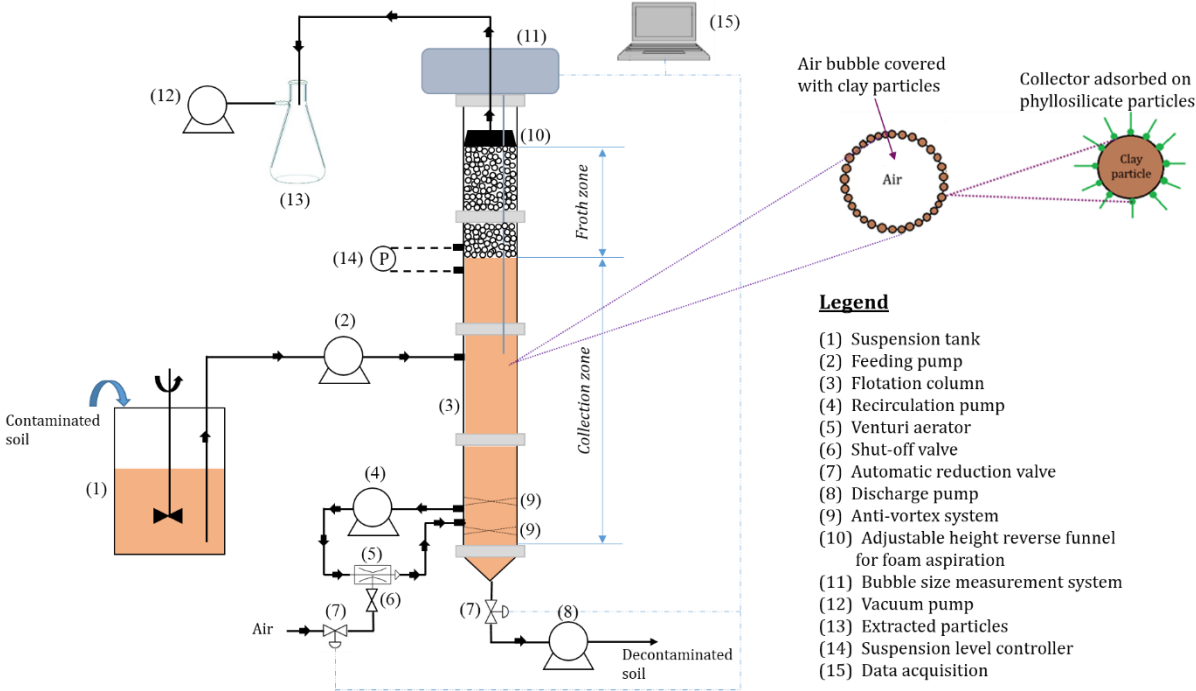


Fig. 1. Scheme of the continuous flotation experimental set-up.

The system operates with a maximum feed flow rate of soil suspension limited at 3.5 L/min. It consists mainly in a monitored column (3) constituted by four superimposed Polyvinyl chloride (PVC) modules of 8 cm diameter and 160 cm height. Soil suspension samples were previously prepared and loaded in the suspension feed tank (1). The column was filled with the soil suspension to be treated by using a peristaltic feeding pump (2). The

suspension was then recirculated at a flow rate of 10 L/min by means of a volumetric pump (4) equipped with a frequency variator in order to avoid the soil particles sedimentation at the bottom of the column. Air was injected at the column bottom, in the 15 cm height aeration region, thanks to a specific aerator (5). The aerator was placed on the recirculation circuit and makes it possible to control, through a mass flow meter, the air flow rate injected into the column. Air flow creates a liquid aeration and the bubbles generation. Two cross-shaped anti-vortex systems (9) were placed at 2.5 cm above and below the air inlet in order to avoid the formation of a vortex and bubble axial clustering. Soil suspension was injected at 60 cm height and had a counter-current contact with rising air bubbles. The collection zone was fixed at 85 cm height. This level was measured by a differential pressure sensor (14) and controlled by a discharge electrovalve (7). Both are connected to a computer interface (15). The interface suspension/froth level was maintained constant by the automatically regulation of the floated suspension flow. The froth continuously generated during the experiment was allowed to stay in the column few minutes (τ residence time in seconds) and then sucked at a define height in the column by a reverse funnel (10) connected to a vacuum pump (12). The funnel height was adjusted to modify the froth residence time in the column before removal. The treated soil was recovered at the bottom of the column by means of a peristaltic discharge pump (8).

In the collection area, the air bubble size was determined using an intrusive bubble sampling system constituted by a long pipe (1 cm diameter and 80 cm length) immersed in the suspension. Bubbles are conveyed up to a lighted viewing chamber (11) on which is focused a high speed camera. All operations are controlled by a computer interface with a LabVIEW software.

2.2.3. Experimental procedure

For a typical experiment, 40 L of soil suspension were prepared 20 min before starting the experiment and kept under continuous stirring. The suspension feed flow rate was fixed at 0.5 L/min for all flotation tests. TTAB was added to the suspension 20 min before introducing the mixture into the column within the required time to have it adsorbed on the surface of the hydrophilic negatively charged fine particles. The air was injected when the collection zone was filled. Flotation was started after aeration. Because the gas hold up was unstable during the first minutes of experiment (when the column was in unsteady-state conditions), data acquisition was started only after 10 min. Four froth heights were successively tested during each experiment. The froth was collected during 10 min at each height and weighted. The collected froth was then dried in an oven at 105°C for 24 h and weighted to evaluate the global separation rate. The global separation rate was calculated according to the following equation:

$$\text{Global separation rate (\%)} = \frac{\text{mass of dried separated particles}}{\text{initial mass of soil}} \times 100 \quad (1)$$

TTAB concentration was expressed as the following ratio:

$$\text{TTAB/soil ratio (\%)} = \frac{\text{mass of TTAB}}{\text{initial mass of soil}} \times 100 \quad (2)$$

The froth water content is defined by the volume liquid fraction (ε) retained in the froth and calculated for each height according to Eq. (3). It is assumed that the injected air entrapped in the froth was entirely conserved all along the experiment.

$$\varepsilon (\%) = \frac{V_{\text{water}}}{V_{\text{water}} + V_{\text{air}} + V_{\text{soil}}} \times 100 = \frac{Q_{\text{water}}}{Q_{\text{water}} + Q_{\text{air}} + Q_{\text{soil}}} \times 100 \quad (3)$$

Where V_i and Q_i represent the volumes and flow rates of water, air and soil.

Scale-up studies were performed, well supported by modeling and by experiments carried out at lab and pilot scales (40 L and 400 L, respectively). The lab flotation column had the

following dimensions: 8 cm of diameter and 160 cm of height, and the pilot column diameter is 20 cm of and the height of 220 cm. The section of the pilot column is multiplied by 6.25. The air flow rate/suspension flow rate ratio and the air superficial velocity were adopted as scale-up criteria. The upscaling studies were performed at the three following operating conditions, where C_s is the soil concentration and τ is the froth residence time in the column:

- *Run 1*: TTAB/soil ratio=0.3%, $C_s=50$ g/L, $\tau=120$ s and air flow rate/suspension flow rate ratio=2.
- *Run 2*: TTAB/soil ratio=0.2%, $C_s=50$ g/L, $\tau=150$ s and air flow rate/suspension flow rate ratio=2.
- *Run 3*: TTAB/soil ratio=0.2%, $C_s=100$ g/L, $\tau=90$ s and air flow rate/suspension flow rate ratio=2.

2.2.4. Controlled parameters and operating conditions

The flotation experiments were conducted over a broad range of experimental conditions. Four parameters were investigated, including TTAB/soil ratio, froth residence time, suspension concentration and air flow rate. The froth residence is calculated by dividing the froth height by the superficial air velocity. The details of the flotation processing parameters investigated in this work as well as their variation ranges are summarized in Table 1.

Table 1

Flotation operating conditions at lab and pilot scales.

Installation	Parameter	Range
	Ratio TTAB/soil	0.1-0.4%

Lab scale	Froth residence time	60-150 s
	Suspension concentration	50-125 g/L
	Air flow rate	0.5-2.5 L/min
	Suspension feed flow rate	0.5 L/min
<hr/>		
	Ratio TTAB/soil	0.2-0.3%
	Froth residence time	90-150 s
Pilot scale	Suspension concentration	50-100 g/L
	Air flow rate	Maintained at 6 L/min
	Suspension feed flow rate	3 L/min
<hr/>		

2.3. Characterization techniques

2.3.1. Particle-size Distribution

To highlight the flotation process efficiency to selectively separate fine particles, particle-size distribution of various floated samples were compared. Particle-size distribution measurements were carried out by laser diffraction on CILAS 1090 analyzer (CILAS, Orléans, France) in Milli-Q® water. Ultrasonication (50 W) was applied to disperse the particles before and during analysis with a total ultrasonication time of 3 minutes. Previous studies showed that size distribution is no longer impacted by ultrasonication after 3 minutes. Particle-size distribution tests were at least duplicated for each condition, and the average values were presented to ensure the repeatability and the accuracy of the experimental data.

2.3.2. Particle-size fractionation

In order to characterize the soil textural properties and to compare the particle-size distribution obtained on separated particles with raw soil (in absence and in presence of TTAB), a particle-size fractionation method was applied, based on the standardized AFNOR NF X 31-107 method. Particle-size fractionation enables to quantify the relative abundance of each grain-size fraction in the sample by separating particles in water according to their size. Samples were divided into 5 fractions, each one having different particle sizes: coarse sand (>200 μm), fine sand (200-50 μm), coarse silt (50-20 μm), fine silt (20-2 μm) and clay (<2 μm), according to the classification of the IUSS. Particle-size fractionation experiments were performed according to the following protocol: 13 g of each sample were suspended into 150 mL of Milli-Q® water and stirred under continuous vibration stirring for 12 h in order to reach a stabilized dispersion state. First, coarse and fine sand particles (>50 μm) were separated by using a wet sieving method with 200 and 50 μm screens meshes. Particles trapped on each screen were collected, dried at 105 °C and weighted. Then, the suspension coming through the 50 μm screen (containing particles <50 μm) was sonicated for 3 min and transferred into a sedimentation cylinder. Particles smaller than the silt size fraction (<50 μm) were further separated by sedimentation according to Stokes' law, given in the following expression [27]:

$$v = \frac{2 r^2 g \Delta\rho}{9 \mu} \quad (4)$$

Where v is the particle velocity, r is the particle radius, $\Delta\rho$ (1.6 g/cm^3) is the density difference between the particles and the fluid, g (9.8 m/s^2) is the gravity acceleration, and μ (10^{-3} Pa.s) is the fluid viscosity.

By this method, it is assumed that the particles have a spherical form and an average density at 2.6 g/mL .

The sedimentation was performed in a graduated 1.2 L glass cylinder filled with 30 cm of suspension at 20 °C. The sampling was performed via a vacuum pump and a pipette positioned at the chosen depth (10 cm below the meniscus of suspension). Calculated settling times 4 min 48 s, and 8 h were respectively assigned to the 20-2 μm and <2 μm particle-size fractions. The 50-20 μm fraction is the final residual fraction, purified from the finest particles. The suspension contained in the cylinder was stirred and placed stand during the required time for sedimentation. The suspension containing <2μm or 2-20μm particles was thus sucked and centrifuged at 10000 rpm for 40 min. This process was repeated five times so that the suspension is depleted of the targeted fraction. Finally, centrifuged solids were dried at 105 °C in an oven and weighted.

2.3.3. X-Ray Diffraction analysis

X-Ray Diffraction (XRD) measurements were performed on XRD 5000 INEL powder X-ray diffractometer using CuK α radiation, equipped with a CPS120 curve detector Si/Li, to analyze the mineral structure of the raw soil and the separated particles. Samples for XRD analysis were prepared by grinding to less than 50 μm sizes (in the case of raw soil) and inserted into sample holder. The XRD powder patterns were recorded during 1h at 30 kV and 30 mA for a Cu-target tube at room temperature of 25 °C. All samples were scanned with a 2 θ angle between 3° and 70° and the patterns were recorded on the whole 2 θ range and cumulated each few seconds during 1h in order to optimize the signal/noise ratio. The data were processed to analyze patterns including the mineral phases identification. Peaks locations and heights were compared with those of standard minerals by means of Match!2 software using the COD-Inorg Rev 81284 database to characterize mineral structures contained in the samples. Minerals quantification was unavailable due to the too complex mineralogical assemblages of samples.

3. Results and discussion

3.1. Raw soil characterizations

Although organic materials may have an influence on mineral particles flotation, we gave higher importance to maintaining the original sample conditions, where organic matter is expressed as particulate organic matter or associated with mineral particles in soil aggregates. Before flotation experiments, a series of granulometric analysis was conducted in order to fractionate particles and quantify the proportion of each fraction in the raw soil used in this study by separating particles in water according to their size. The particle-size distribution of the raw soil is listed in Table 2. There is a wide range of particle-size distribution that confers to this soil an equilibrated texture. According to its position in the soil textural diagram [28], the soil was classified as loamy soil. It shows a dominance of the silt fraction 20-50 μm . The raw soil have an acidic character, its pH is equal to 5.5, measured in water based on the standardized AFNOR NF ISO 10390 method.

Table 2

Textural characterization of the raw soil used in this study.

	Clay		Silt		Sand
size	0-2 μm	2-20 μm	20-50 μm	50-200 μm	200-2000 μm
weight percent	11.28	18.70	35.67	22.29	13.04

Identification of the different minerals present in the raw soil was performed on the XRD diffractogram acquired on the raw soil, shown in Fig. A in supplementary material. It is clear from this figure that soil is a complex system; numerous structures were identified and expressed in various amounts (various peak intensities). Six negatively charged structures

were identified: four phyllosilicate clays (illite, montmorillonite, kaolinite and chlorite), quartz and feldspar. These negatively charged phases are able to adsorb cationic collector to become more hydrophobic and thus they can be floated and separated from soil. Other hydrophilic and/or positively charged particles were identified in the raw soil (i.e., goethite, calcite, iron aluminum oxide hydroxide, gypsum).

3.2. Impact of process parameters upon the separation performance

In column flotation, the separation of fine particles from soil is significantly affected by the processing variables related to: (1) collector concentration (TTAB/soil ratio), (2) froth residence time (τ), (3) feed suspension concentration (C_s), and (4) gas dispersion, such as air flow rate (Q_{air}) (or superficial air velocity (J_g)). This issue is addressed in the following subsections.

3.2.1. Impact of collector concentration

The impact of collector concentration, as one of the key variables that affect the transport phenomena occurring during the flotation process, on the separation rate was examined at $\tau=120$ s, $C_s=50$ g/L and $Q_{air}=1$ L/min. Flotation results are depicted in Fig. 2, showing the global separation rate plotted against TTAB/soil ratio. It is worth noting that the separation rate is highly sensitive to the collector concentration; it increases drastically from 5% to 70% when the TTAB/soil ratio was raised from 0.1 to 0.4%.

In the case of negatively charged particles, increasing cationic TTAB collector concentration increases the cationic compensation of the particles surface charge by TTAB and therefore changes their surface properties by electrostatic adsorption. On one side, the surface becomes more hydrophobic and the affinity to air bubbles increases, leading to an enhancement of particles attachment to the bubble surface due to hydrophobic interaction. On the other side, negative surface charges are dominantly compensated by the surfactant which

contributes to smallest particles aggregation and therefore improve their capture probability by bubbles [29].

Nonetheless, it is interesting to note that a further increase of the TTAB/soil ratio beyond 0.4% does not result in a perceptible improvement in the separation rate. On the contrary, at TTAB/soil ratios above 0.4%, an instable hydrodynamic system characterized by the disappearance of the suspension/froth interface and multidirectional particles movement was observed. Above this TTAB/soil ratio, the venturi aerator generated very small air bubbles, stabilized by free TTAB (TTAB not adsorbed on particles), that were not able to rise up to the suspension surface and accumulate in the column which generates random movements. So, 0.4% can be considered as a critical TTAB/soil ratio, a ratio not to be exceeded to have a stable hydrodynamic flotation with a well-defined suspension/froth interface.

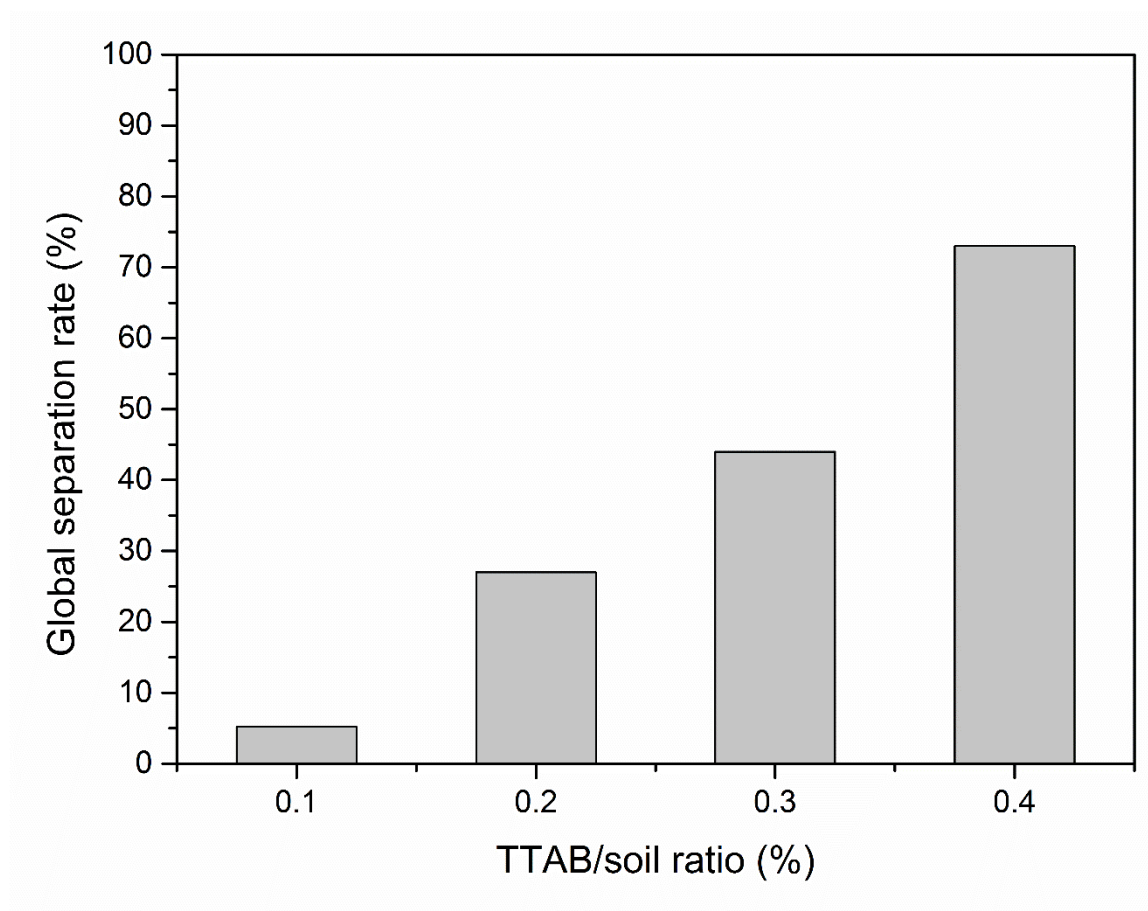


Fig. 2. Impact of collector amount on the global separation rate. Global separation rate versus TTAB/soil ratio at $\tau=120$ s, $C_s=50$ g/L and $Q_{air}=1$ L/min.

To study the process selectivity to fine particles and identify the specific information on the morphology and particle-size distribution of the separated particles at each TTAB/soil ratio, laser granulometry analysis were performed on samples floated at the different TTAB/soil ratios (0.1, 0.2, 0.3 and 0.4%). Particle-size distributions of the separated particles are compared in Fig. 3. Particle-size distribution of the raw soil sieved at 200 μm is also reported as reference curve. Results revealed that the separated particles at different TTAB/soil ratios present distinctly different size distributions. Particles from 1 μm to 100 μm were transferred into the froth. Three main particle-sizes are detected for the separated particles samples: a minor particle-size centered at 3 μm which can be mainly attributed to phyllosilicates [29], and two major particle-sizes centered at 10 μm and 30-50 μm (depending on flotation conditions). The first major particle-size could be dominated by phyllosilicate aggregates [29] and the second one could be composed by a phyllosilicate and quartz mixture. Furthermore, it can be seen from the figure that the particle-size distribution shifted towards small particle diameters when the TTAB/soil ratio was decremented from 0.4 to 0.1%. So, the lower the TTAB/soil ratio, the more size-selective is the separation. Particles can be transported from suspension to froth by two competing phenomena: attachment to bubble and entrainment. This last phenomenon is totally unselective and may collect large particles (both hydrophobic and hydrophilic particles) [30]. It was shown that entrainment is amplified at high froth liquid fraction which is in turn amplified at high collector concentration [31]. This could explain the removal of larger particles at higher TTAB/soil ratios.

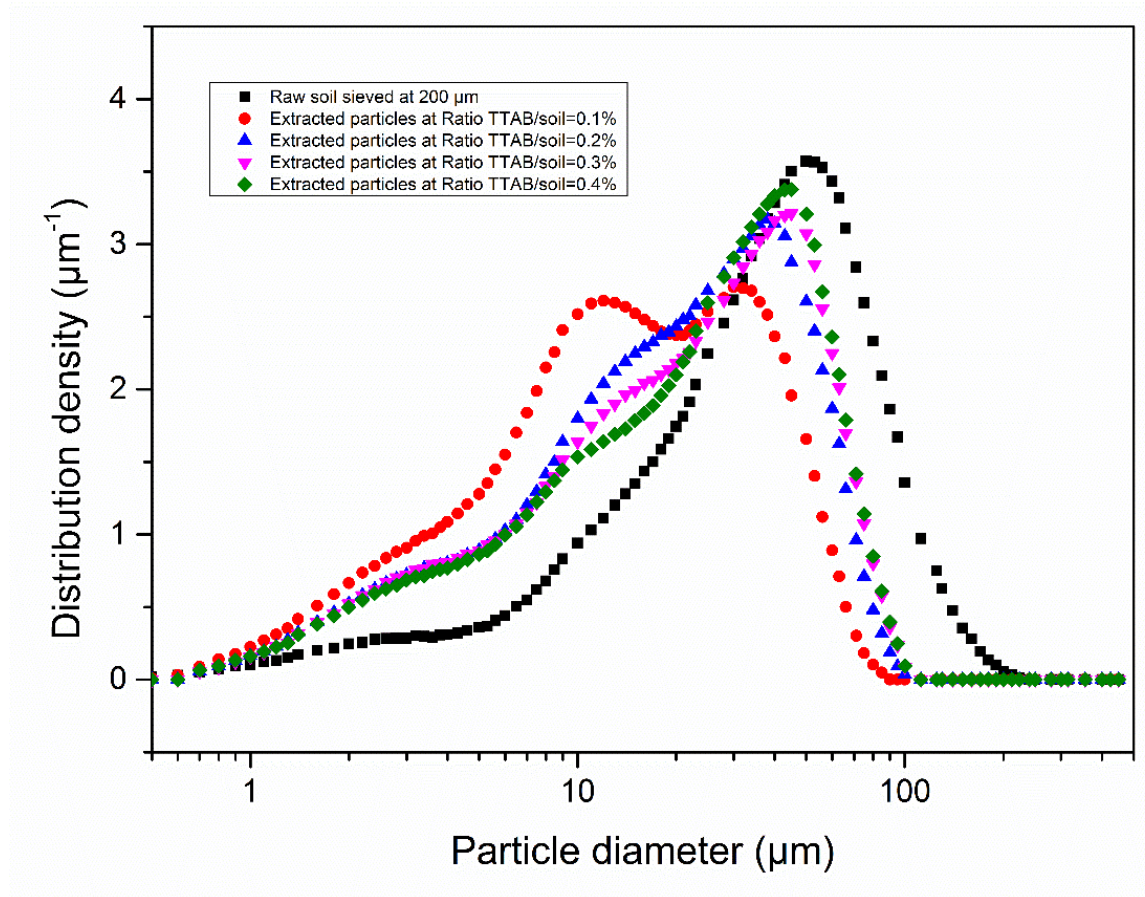


Fig. 3. Particle-size distribution of the froths particles separated at different TTAB/soil ratios.

As discussed above, the separation performance strongly depends on the collector concentration, but other parameters affecting the separation rate are also to be considered.

3.2.2. Impact of froth residence time

This part evaluates the effect of froth residence time over the separation performance at a broad range of experimental conditions. Twelve flotation tests were conducted at residence times between 60 and 150 s and at three different TTAB/soil ratios (0.1, 0.2 and 0.3%). Experiments were performed at a suspension concentration of 50 g/L and an air flow rate of 1 L/min. Fig. 4 presents the relationship between froth residence time and separation rate at different TTAB/soil ratios. It can be noticed that at a fixed TTAB/soil ratio, the residence time increase penalized the separation rate. All profiles follow the same trend, with a slope increasing with TTAB/soil ratio. For example, at given TTAB/soil ratio of 0.2%, a noticeable

rate loss from 52 to 27% was observed when the froth residence time is doubled from 60 to 120 s.

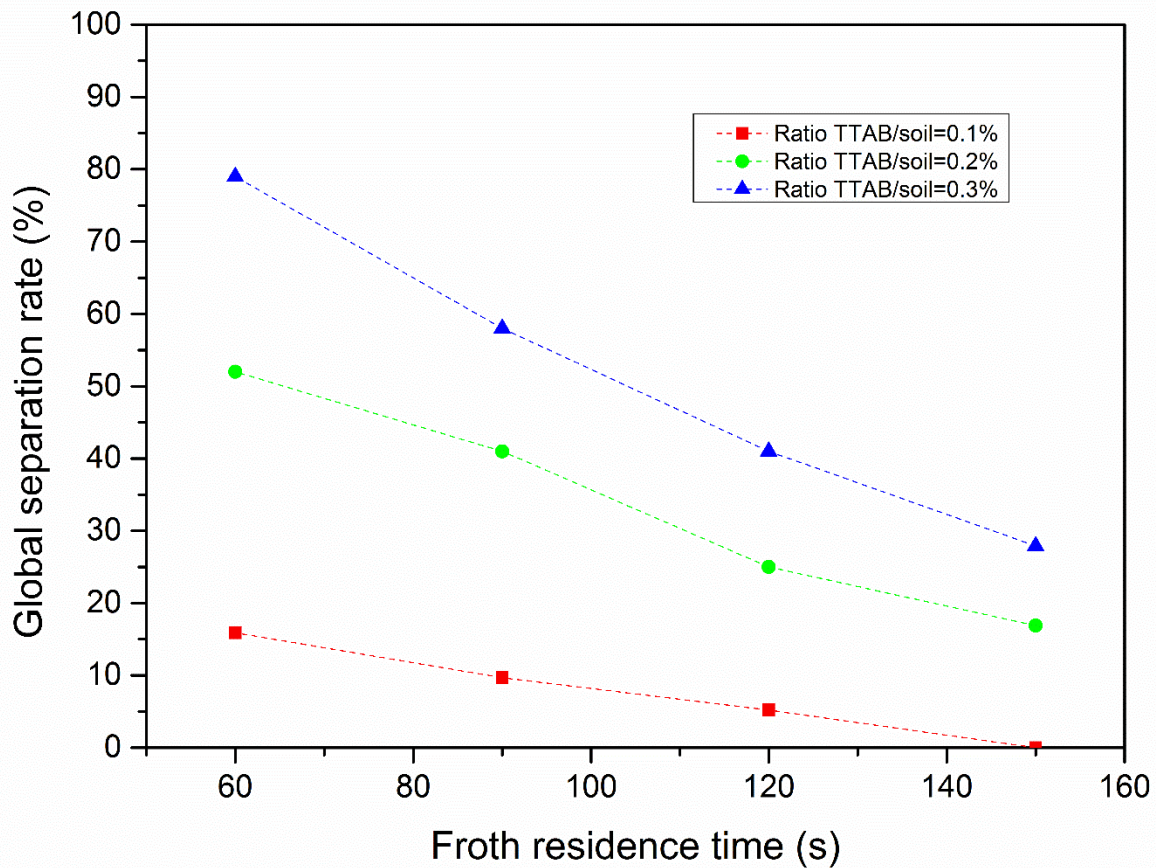


Fig. 4. Global separation rate versus residence time at different TTAB/soil ratios.

The separation rate decreases classically with the froth residence time. Indeed, ~~It is well-known that~~ the froth particulate flotation mechanism involves three essential phenomena: (1) attachment of the particle to air bubble or the so-called true flotation, (2) entrainment and (3) drainage [26, 29, 32]. The two first elementary processes, (1) and (2), occur in the collection zone (suspension zone), whereas the third one occurs in the froth zone. ~~The cleaning zone-~~ **In the froth zone,** ~~is dynamic and subject to free water~~ **gravitational drainage occurs** which leads to liquid film thinning, in which interfacial forces become important governing further stability of the liquid film between the gas-liquid and solid-liquid interfaces [33]. Particles can be entrained by the water flow or remain attached to air bubbles and form aggregates which

can slowdown the water drainage [34]. In our case, the higher the residence time, the greater is the drainage duration and thus the lower is the separation rate. The drainage in the froth allows to get rid of the unattached entrained particles and froth is selective of the attached particles as usually observed in the literature [35-37]. Rahman et al. [35] noted in their study on the effect of flotation variables on the recovery of different silica particle size fractions, a strong effect of froth residence time upon the separation rate and the size distribution of the recovered particles. They attributed this behavior to the detachment of particles at higher froth residence times (higher froth depths).

~~Accordingly, the disadvantageous effect of residence time on the separation rate could be mainly related to the drainage phenomenon.~~

In order to evaluate more precisely the drainage phenomenon efficiency, a set of froth liquid fraction (ε) measurements was performed at two TTAB/soil ratios (0.2 and 0.3%) and several residence times (between 60 and 150 s). Froth liquid fractions (ε) were calculated according to Eq. (3) described in the experimental section. The ε values measured on froths obtained at these conditions are tabulated in Table 3. It can be noted that at equivalent TTAB/soil ratio, the longer the residence time the lower is the froth liquid fraction. Relatively dry froths were obtained at higher residence times, but froths became more humid below a residence time of 60 s with liquid fraction values reaching 4.0 and 5.1% at TTAB/soil ratios of 0.2 and 0.3%, respectively.

The froth liquid fraction decrease, along with a residence time increase, emphasizes the drainage process and consequently particles entrainment downstream.

Another important point to be highlighted is the fact that, at a given residence time, froth liquid fraction values obtained at 0.2% of TTAB/soil ratio are lower than those obtained at a ratio of 0.3%. It confers to the froths made with a TTAB/soil ratio of 0.2% a potentially better

stability than those obtained at TTAB/soil ratio of 0.3%. Most likely, that is why the effect of froth residence time on the separation rate is more pronounced at higher TTAB/soil ratios.

Table 3

Froth volume liquid fraction (%) obtained at different residence times.

Ratio TTAB/soil (%)	Froth residence time (s)			
	60	90	120	150
0.2	4.0	1.5	0.9	0.7
0.3	5.1	2.4	1.3	1.0

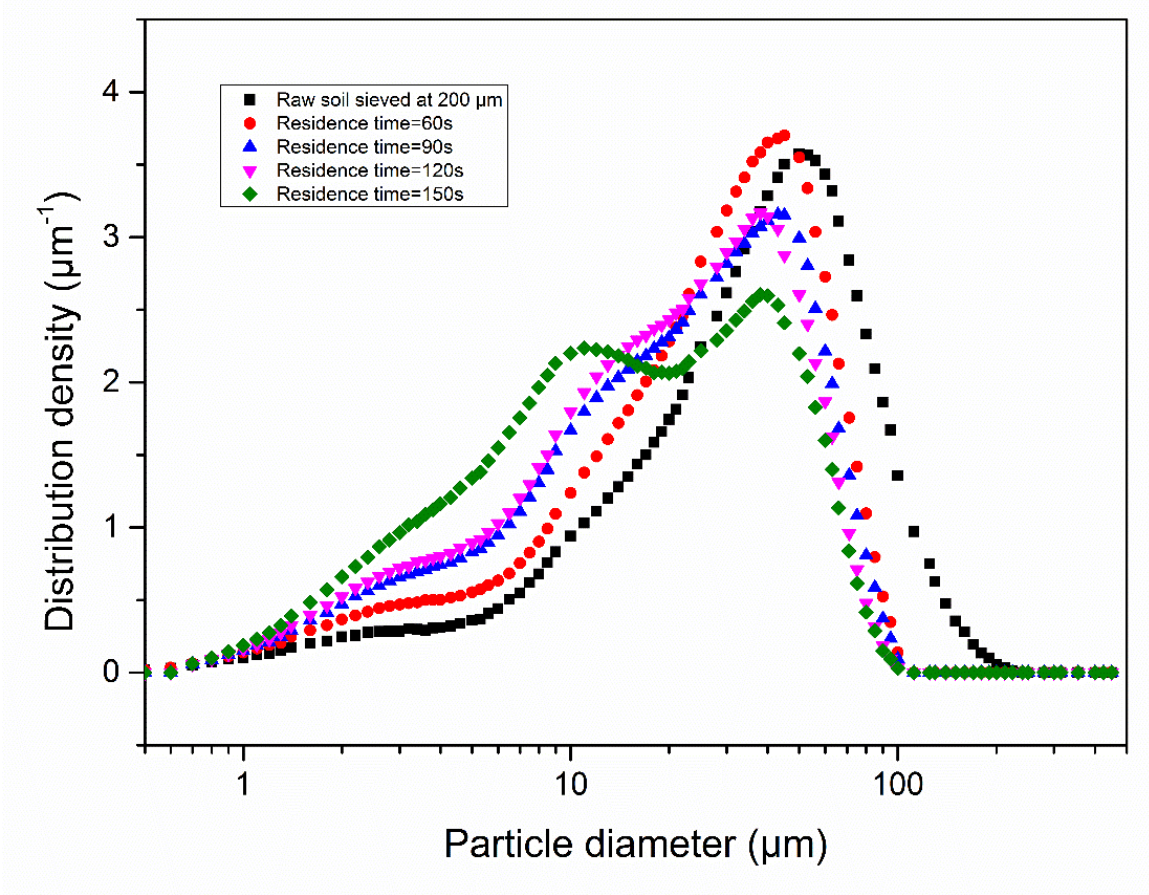


Fig. 5. Particle-size distribution of the froths particles separated at different residence times with 0.2% TTAB/soil ratio.

Fig. 5 compares the particle-size distributions of the froths particles separated with a ratio TTAB/soil of 0.2% and collected at four residence times (60, 90, 120 and 150 s). The results indicated that the particle-size distribution shifted towards the smallest sizes and the mean particle diameter decreased when the residence time was incremented from 60 to 150 s. This behaviour could be attributed to the detachment of the heaviest particles or the particles badly attached (particles having an incomplete hydrophobization). This confirms the finding that the drainage process led to remove the large particles from the froth stream, resulting in a selective separation of the smallest ones.

~~The observed effects of the froth residence time on the separation rate and the size distribution of the separated particles are in agreement with the literature [35-37]. In their study on the effect of flotation variables on the recovery of different silica particle size fractions, Rahman et al. [35] noted a strong effect of froth residence time upon the separation rate and the size distribution of the recovered particles. They attributed this behavior to the detachment of particles at higher froth residence times (higher froth depths).~~

To conclude this part of the impact of froth residence time, increasing the froth residence time would enhance the drainage phenomenon, thereby decreasing the separation rate and enhancing the separation size-selectivity.

3.2.3. Impact of suspension concentration

In the experiments described above, the feed suspension concentration was 50 g/L. In order to examine the impact of suspension concentration on the separation rate, a series of experiments was carried out at four suspension concentrations: 50, 75, 100 and 125 g/L, and at different froth residence times (90, 120 and 150 s). These experiments were performed at $Q_{air}=1$ L/min and TTAB/soil ratio=0.2%. Fig. 6 presents the separation rate evolution as a function of the suspension concentration obtained at the several residence times studied. It is

clear that, at a fixed residence time, a significant rate gain was noticed when the suspension concentration is increased from 50 to 100 g/L. More stable froths were formed when increasing suspension concentration from 50 to 100 g/L. The improvement of collision (particle/air bubble) and capture probability at higher suspension concentrations was thought of as a possible explanation leading to the formation of heavily charged froths at 100 g/L, stabilized by fine particles.

It could be furthermore observed from this illustration that the separation rate is more sensitive to suspension concentration at prolonged froth residence times. Indeed, with the same residence time increase, the separation rate gains the maximum change at higher residence times, especially when the suspension concentration was doubled from 50 to 100 g/L.

Another noteworthy aspect from the plot illustrated in Fig. 6 emerges from the comparison between the separation rates obtained at 100 and 125 g/L at each froth residence time. Indeed, an additional increment of suspension concentration from 100 to 125 g/L showed no farther significant rate enhancement whatever the residence time. The air bubbles saturation with particles may be responsible for this observation.

A similar trend was observed by Luo et al. [38] in their work about the investigation of the critical importance of pulp concentration on the flotation of galena from a low grade lead–zinc ore. Authors noted that the recovery of galena minerals increases drastically with the pulp concentration at lower concentrations to reach a plateau at higher pulp concentrations.

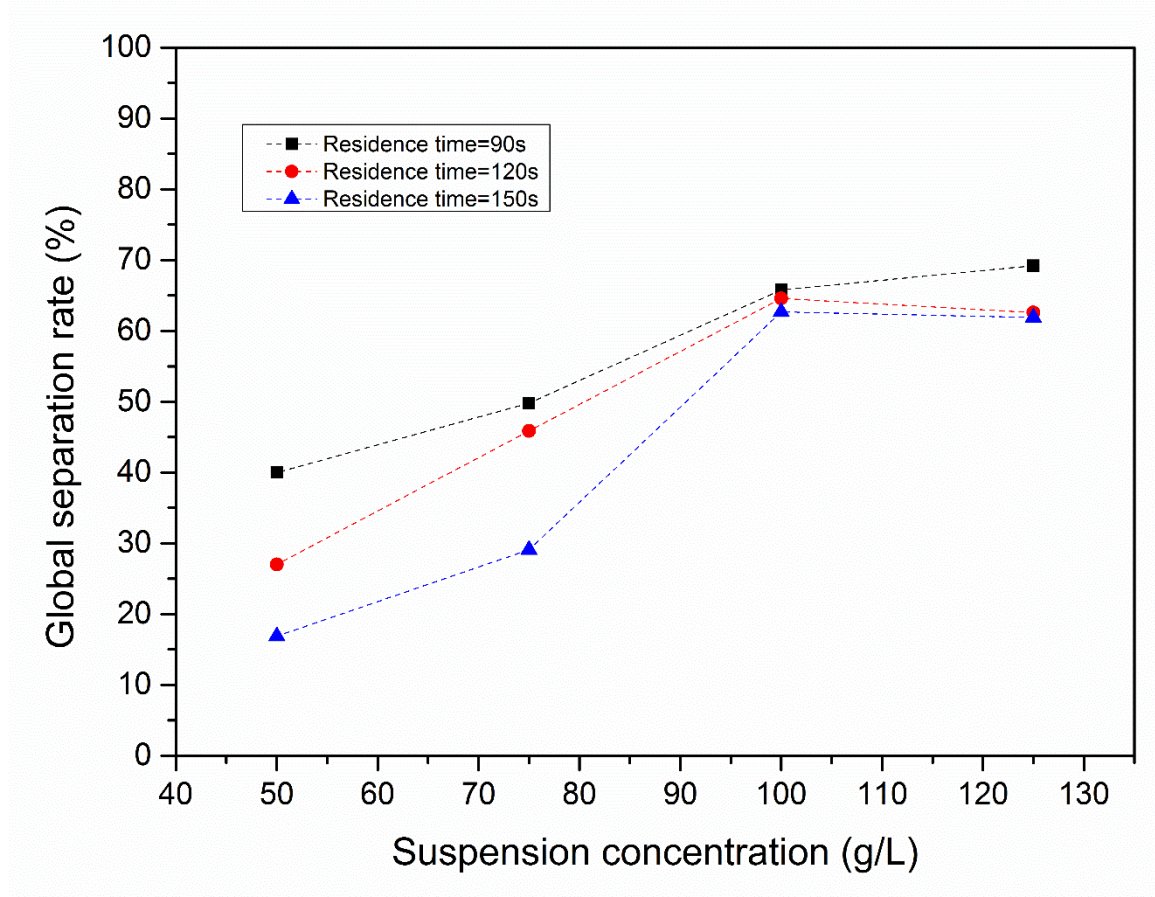


Fig. 6. Impact of suspension concentration on the global separation rate. Global separation rate versus suspension concentration at different residence times.

3.2.4. Impact of air flow rate

Concerning the air flow rate study over the separation behavior, various flotation experiments were conducted at five air flow rates: 0.5, 1, 1.5, 2 and 2.5 L/min. The resulting air superficial velocities were: 9.9, 19.8, 29.8, 39.7 and 49.7 cm/min, respectively. Air superficial velocities were calculated by dividing the volumetric air flow rate by the cross-sectional area of the column. It is worth noting that the other flotation parameters were fixed, namely $\tau=120$ s, $C_s=50$ g/L and TTAB/soil ratio=0.2%. The influence of air flow rate on the separation rate is shown in Fig. 7. Based on these results, it is important to underline that the separation rate considerably increased when air flow rate was raised from 0.5 to 1.5 L/min, especially from 0.5 to 1 L/min where the separation rate is multiplied by a factor of 2.5. This is in agreement with literature: many authors observed that the separation rate increases significantly with air superficial velocity and attributed this behavior to the increase of the air bubbles number and the enhancement of the particle/bubble collision and capture probability [39, 40]. Moreover a

larger increase of the air flow rate (from 1.5L/min to 2.5L/min), corresponding to intermediate air superficial velocity from 29.8 to 49.7 cm/min, has no more effect onto the global separation rate as shown on Fig. 7. The separation rate reached a maximum around 1,5-2 L/min. This was previously observed in literature for chalcopyrite : after a plateau value, a drop of the separation rate at higher superficial velocities due to high bubbles coalescence was described at higher air flow rate (over 6L/min when superficial velocity exceeds 120 cm/min) [41]. In our case, it means that coalescence of the bubbles seems to start around 1,5L/min and leads to a decrease of the bubbles surface area where particles can be attached and a limitation of the global separation rate, even if the amount of gas increase into the column.

~~In literature, many authors observed that the separation rate increases significantly with air superficial velocity and attributed this behavior to the increase of the air bubbles number and the enhancement of the particle/bubble collision and capture probability [39, 40]. They described a drop in the separation rate at higher superficial velocities (when superficial velocity exceeds 120 cm/min) due to bubbles coalescence [41].~~

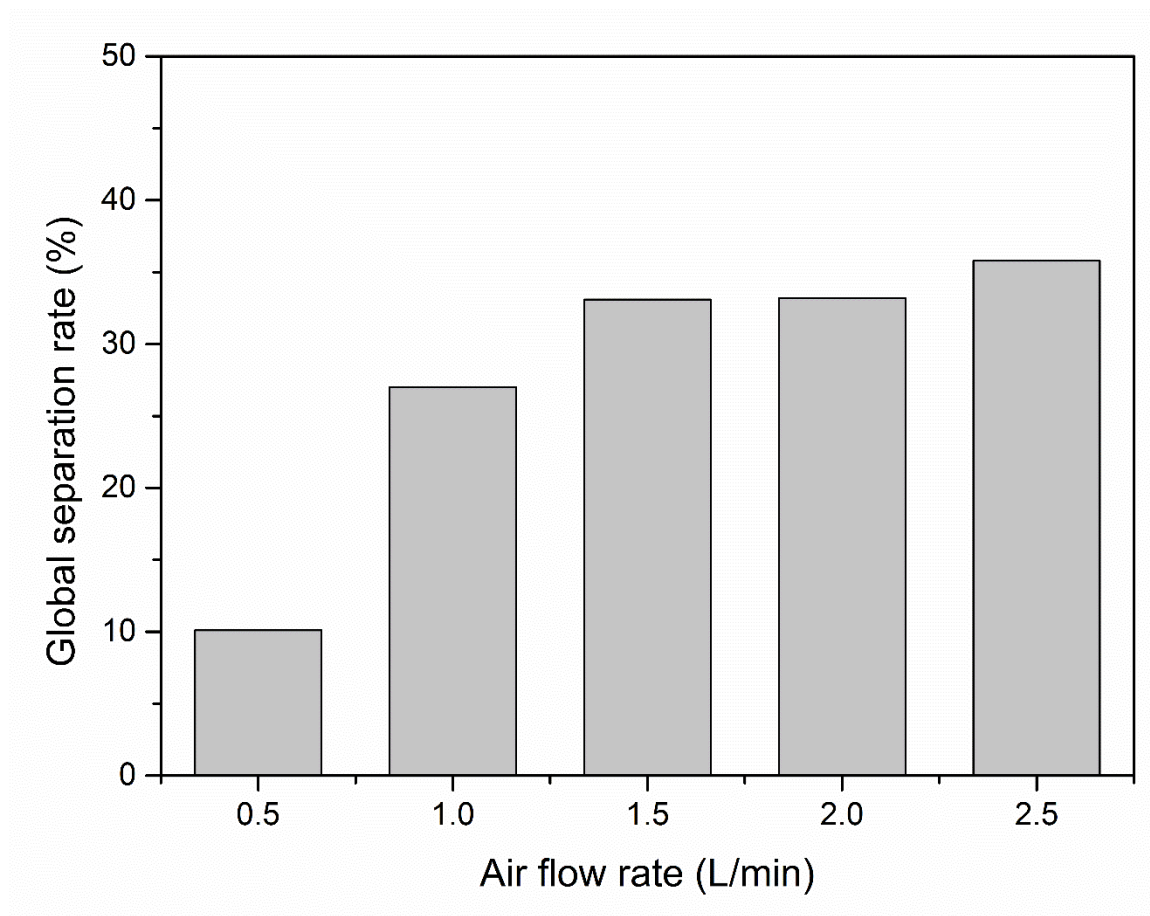


Fig. 7. Impact of air flow rate on the global separation rate at $\tau=120$ s, $C_s=50$ g/L and TTAB/soil ratio=0.2%.

3.3. Determination of partial separation rates

Particle-size fractionation analysis, applied on the raw soil and the froth particles, was investigated in order to identify the specific information on the partial separation rates. The results are presented in Fig. 8. The analyzed froth sample was floated at the following conditions: TTAB/soil ratio=0.3%, $\tau=120$ s, $C_s=50$ g/L and $Q_{air}=1$ L/min. In order to disclose an impact of the collector on the initial soil particle-size distribution, the same analysis was carried out on the raw soil in presence of TTAB collector (soil + 0.3% TTAB). Based on these findings illustrated in Fig. 8, the most relevant insights that can be noticed are as follows. The raw soil exhibits a predominance of the 20-50 μm fraction with a relative abundance of 35%. The presence of TTAB collector introduced before flotation process did not significantly alter the particle size distribution of the raw soil. An enrichment of the 2-20 μm and 20-50 μm fractions was measured in the froth sample: rise of 22% for the 2-20 μm fraction and 39% for the 20-50 μm fraction. Whereas, a depletion of the fraction <2 μm and especially the fraction > 200 μm in the froth sample was noted. For the 50-200 μm fraction, a slight enrichment was observed. As demonstrated by laser diffraction granulometry (Figs. 3 and 5), there are no particles greater than 100 μm in the froth and therefore the 50-200 μm fraction (measured according to the standardized classification of the IUSS) depicts actually the 50-100 μm fraction.

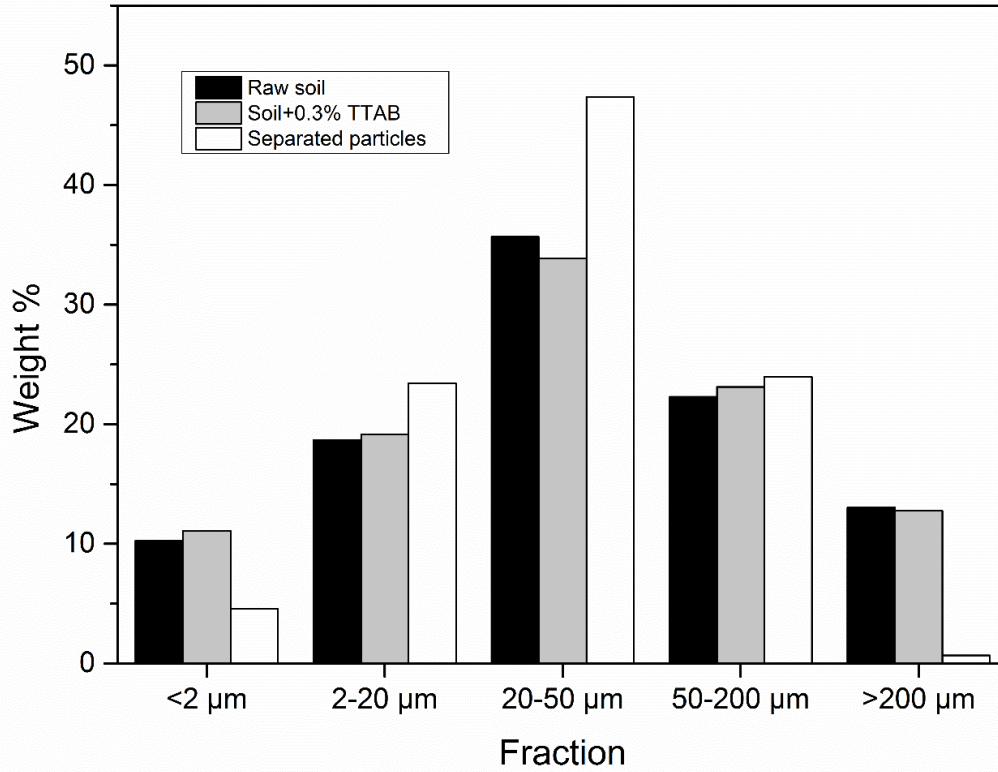


Fig. 8. Particle size distributions according five fractions of raw soil, soil+TTAB and separated particles.

Fig. 9 is extracted from Fig. 8, presenting the separation rates per granulometric fraction (or partial separation rates). The partial separation rates were calculated via the following equation:

$$\begin{aligned}
 \text{Partial separation rate (\%)} &= \frac{\text{mass of the class } i \text{ in the froth}}{\text{mass of the class } i \text{ in the raw soil}} \times 100 \\
 &= \frac{\text{mass percentage of the class } i \text{ in the froth}}{\text{mass percentage of the class } i \text{ in the raw soil}} \\
 &\quad \times \text{Global separation yield} \tag{5}
 \end{aligned}$$

The profile of partial separation rate follows the same trend than that of the grain-size distribution. The 2-20 μm, 20-50 μm and 50-100 μm fractions (presented as 50-200 μm in Fig. 9) were mostly separated with partial separation rates of 55%, 58.5% and 47%,

respectively. The fraction $<2\ \mu\text{m}$ is poorly removed: only 20% of particles $<2\ \mu\text{m}$ were transferred to the froth. This could be explained by the fact that the finest particles do not have sufficient kinetic energy to cross the streamlines created by the bubbles [34] or remain aggregated into larger particle-size. Another possible explanation could be the fact that the finest particles have too much kinetic energy to be adsorbed onto bubbles.

These findings emphasize the process selectivity to particles between 2-100 μm .

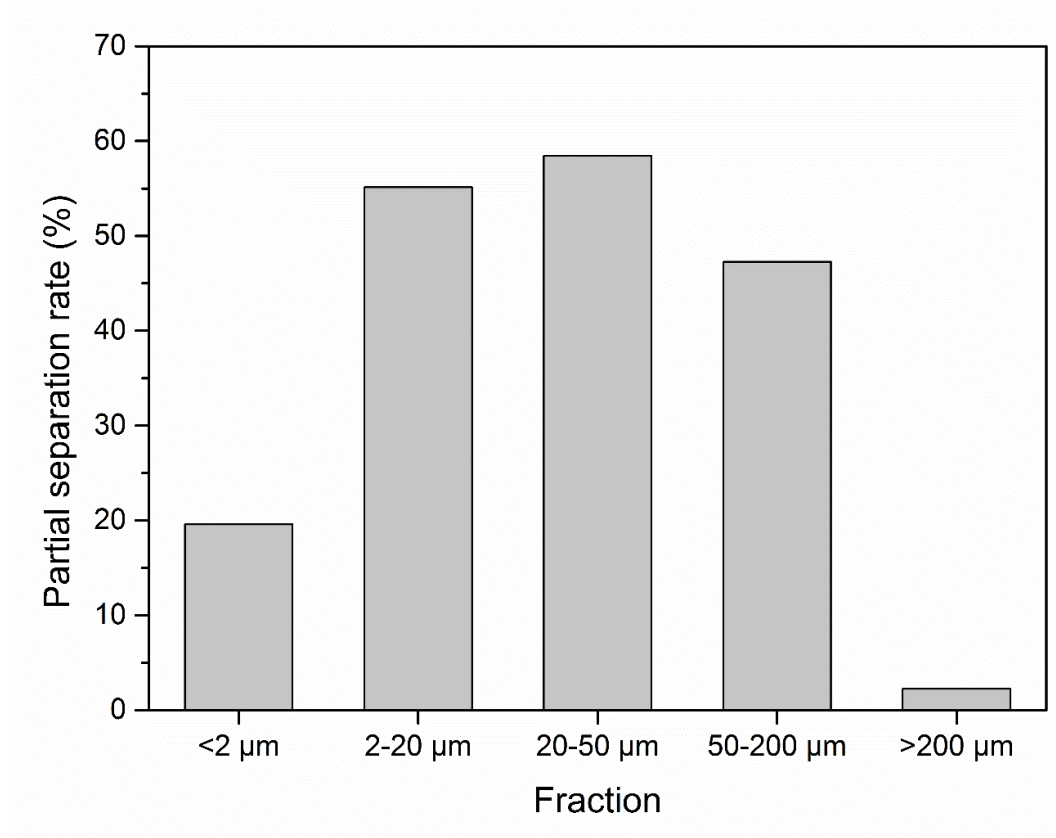


Fig. 9. Separation rates per granulometric fraction.

3.4. Identification of the separated structures

XRD analysis were conducted on froth sample in order to identify the mineralogical structures of floated particles. Fig. B presented in supplementary material shows the XRD pattern acquired on 2-20 μm froth fraction. Pattern analysis indicated a large abundance of

well crystallized quartz (silica). Froth particles contain phyllosilicates, identified as kaolinite, illite, montmorillonite and chlorite, known to entrap trace metals.

Organic matter content was determined in each sample (raw soil, separated particles in the froth and treated soil) by mass loss obtained after calcination at 950°C during 4 h of dehydrated samples. The mass loss by calcination at 950 °C includes destruction of organic matter and calcium carbonate. However, this acidic soil type is originally devoid of calcium carbonates, given that original host rock is a granitic formation. The obtained results are: 7.5% in the raw soil, 4.2% in the froth and 20.9% in the treated soil. In the treated soil (unfloated soil), organic matter content is three times higher than in the raw soil. It is present in these two samples as humic substances and particulate organic matter. Likewise, organic matter taking stems form (plant debris) was observed in the raw and treated soils. The froth contains the lowest organic matter content, which indicates that particulate organic matter is excluded from the froth. Moreover, this floated organic matter is contained as organo-mineral complexes and/or organic particles smaller than 50 µm.

3.5. Scaling-up

Comparison between flotation results obtained at lab scale and those obtained at pilot scale is given in Fig. 10. The differences observed in some separation rates may be explained by the differences between the systems used to inject air bubbles in the column. Indeed, in the lab scale, one aerator was used to introduce air into the column, whereas in the pilot scale two aerators were employed to inject air bubbles and limit sedimentation in the collection zone. The results obtained at lab and pilot scales evidenced a global good agreement, which legitimates the validity of the adopted scale-up criteria and provides valuable evidence to support the technical viability of the soil flotation process for future exploitation at industrial scale. The recommended scale-up criteria in such case is therefore the constancy of the air flow rate/suspension flow rate ratio and the air superficial velocity.

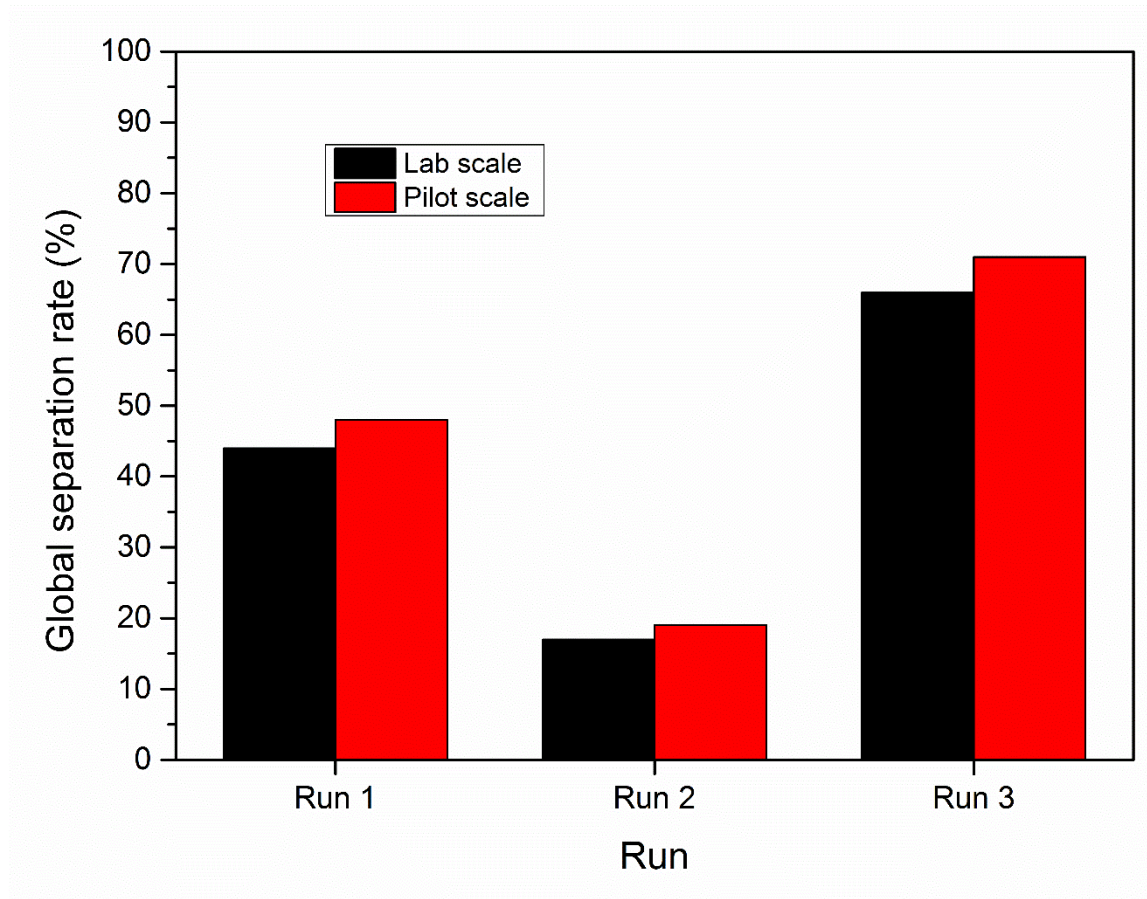


Fig. 10. Comparison of flotation results obtained at lab and pilot scales.

4. Conclusion

This study exhibits a new direction for soil decontamination by separating fine particles carrier of contamination using the flotation technology. A continuous particulate froth flotation process, as an environmentally friendly and cost-effective process, was employed in this present work to separate negatively charged particles, including phyllosilicates, from raw soil. Comparison between separation rates at different collector concentrations indicates that the separation performance strongly depends on TTAB/soil ratio. Using granulometry and XRD analysis, it was showed that phyllosilicate aggregates are transferred into the froth, but other bigger particles are removed such as silica particles (Quartz). The global separation rate depends on the structures of initial negatively charged particles in the soil.

Flotation was performed through a wide range of experimental conditions in order to investigate and understand the influence of the key processing parameters on the separation performance. This work illustrates the feasibility and the potentialities of the flotation technology in a continuous operation mode to separate selectively the fine particles (<100 μm) from soil. The parametric study of the process demonstrates that TTAB/soil ratio, froth residence time and suspension concentration were the most significant parameters that affect the global separation rate. TTAB/soil ratio has a positive effect on the separation rate and a negative effect on the separation size-selectivity, whereas the froth residence time penalizes the separation rate and enhances the selectivity to fine particles.

The upscaling studies evidenced good agreement between results obtained at lab and pilot scales, which legitimates the validity of the adopted scale-up criteria and provides valuable evidence to support the technical viability of the soil flotation process for a future exploitation at industrial scale.

Acknowledgements

The authors gratefully acknowledge D. Beneventi and J. Chapelain from UMR CNRS 5518 (CNRS-Grenoble INP-Agefpi) for technical collaboration to design lab flotation column and VEOLIA and ORANO, for their technical and financial support to this work, in the framework of the French "Programme d'Investissements d'Avenir" (ANR-11-RSNR-0005 DEMETERRES).

References

[1] Ishii, K., A. Terakawa, S. Matsuyama, A. Hasegawa, K. Nagakubo, T. Sakurada, Y. Kikuchi, M. Fujiwara, H. Yamazaki, H. Yuhki, S. Kim, I. Satoh, Measures against Radioactive Contamination Due to Fukushima First Nuclear Power Plant Accidents Part I:

Removing and Decontamination of Contaminated Soil, International Journal of PIXE 22 (2012) 13-19.

[2] Y. Yuki, K. Sekiya, N. Nomura, F. Mishima, Y. Akiyama, S. Nishijima, Study on Volume Reduction of Contaminated Soil by Radioactive Cesium Using Magnetic Separation, IEEE Transactions on Applied Superconductivity 25 (2014) 1-5.

[3] D. Ding, Z. Zhang, Z. Lei, Y. Yang, T. Cai, Remediation of radiocesium-contaminated liquid waste, soil, and ash: a mini review since the Fukushima Daiichi Nuclear Power Plant accident, Environmental Science and Pollution Research 23 (2015) 2249-2263.

[4] S. Djedidi, K. Kojima, H. Yamaya, N. Ohkama-Ohtsu, S.D. Bellingrath-Kimura, I. Watanabe, T. Yokoyama, Stable cesium uptake and accumulation capacities of five plant species as influenced by bacterial inoculation and cesium distribution in the soil, Journal of Plant Research 127 (2014) 585–597.

[5] H. Tsukada, A. Takeda, S. Hisamatsu, J. Inaba, Concentration and specific activity of fallout ^{137}Cs in extracted and particle-size fractions of cultivated soils, Journal of Environmental Radioactivity 99 (2008) 875-881.

[6] F.R. Livens, M.S. Baxter, Particle size and radionuclides levels in some west Cumbrian soils, The Science of the Total Environment 70 (1988) 1-17.

[7] Japan Atomic Energy Agency (JAEA), Decontamination Technology Demonstration Test Project-2 (2012) 7-8. Available from: https://fukushima.jaea.go.jp/english/decontamination/pdf/3-2%20Decontamination_Technology_Demonstration_Test_Project-2.pdf

[8] S. Faure, M. Messalier, Method for the radioactive decontamination of soil by dispersed air flotation foam and said foam, Patent WO2013167728, 2013-11-14.

- [9] K. Murota , T. Saito, S. Tanaka, Desorption kinetics of cesium from Fukushima soils
Journal of Environmental Radioactivity 152 (2016) 134-140.
- [10] M.S. Lutandula, B. Maloba, Recovery of cobalt and copper through reprocessing of tailings from flotation of oxidized ores, Journal of Environmental Chemical Engineering 1 (2013) 1085–1090.
- [11] J. Tian, H. Gao, J. Guan, Z. Ren, Modified floc-flotation in fine sericite flotation using polymethylhydrosiloxane, Separation and Purification Technology 174 (2017) 439-444.
- [12] P.E. Poha, W.Y.J. Onga, E.V. Laub, M.N. Chong, Investigation on micro-bubble flotation and coagulation for the treatment of anaerobically treated palm oil mill effluent (POME), Journal of Environmental Chemical Engineering 2 (2014) 1174–1181.
- [13] M.A.S. Barrozo, F.S. Lobato, Multi-objective optimization of column flotation of an igneous phosphate ore, International Journal of Mineral Processing 146 (2016) 82-89.
- [14] W. Liu, D. Wei, M. Li, Q. Zhao, S. Xu, Synthesis of N,N-Bis(2-hydroxypropyl)laurylamine and its flotation on quartz, Chemical Engineering Journal 309 (2017) 63–69.
- [15] D.S. Patila, S.M. Chavana, J.U. Kennedy Oubagaranadin, A review of technologies for manganese removal from wastewaters, Journal of Environmental Chemical Engineering 4 (2016) 468–487.
- [16] C.Q. Wang, H. Wang, J.G. Fu, Y.N. Liu, Flotation separation of waste plastics for recycling-A review, Waste Management 41 (2015) 28–38.

- [17] D.E. Tsatsis, D.K. Papachristos, K.A. Valta, A.G. Vlyssides, D.G. Economides, Enzymatic deinking for recycling of office waste paper, *Journal of Environmental Chemical Engineering* 5 (2017) 1744–1753.
- [18] S. Vashisth, C.P.J. Bennington, J.R. Grace, R.J. Kerekes, Column flotation deinking: State-of-the-art and opportunities, *Resources, Conservation and Recycling* 55 (2011) 1154-1177.
- [19] Y. Suzuki, N. Hanagasaki, T. Furukawa, T. Yoshida, Removal of Bacteria from Coastal Seawater by Foam Separation Using Dispersed Bubbles and Surface-Active Substances, *Journal of Bioscience and Bioengineering* 105 (2008) 383–388.
- [20] B.P. Binks, T.S. Horozov, *Colloidal Particles at Liquid Interfaces*, Cambridge University Press, New York, 2006.
- [21] L.C. Goldenberg, I. Hutcheon, N. Wardlaw, Experiments on transport of hydrophobic particles and gas bubbles in porous media, *Transport in Porous Media* 4 (1989) 129–145.
- [22] Z.Q. Huang, H. Zhong, S. Wang, L.Y. Xia, G.Y. Liu, Comparative studies on flotation of aluminosilicate minerals with Gemini cationic surfactants BDDA and EDDA, *Transactions of Nonferrous Metals Society of China* 23 (2013) 3055-3062.
- [23] H. Jiang, L.H. Xu, Y.H. Hu, D.Z. Wang, C.K. Li, W. Meng, X.J. Wang, Flotation and adsorption of quaternary ammonium cationic collectors on diasporite and kaolinite, *Nonferrous Metals Society of China* 21 (2011) 2528-2534.
- [24] L.I. Xia, H. Zhong, G.I. Liu, Z.Q. Huang, Q.W. Chang, X.G. Li, Comparative studies on flotation of illite, pyrophyllite and kaolinite with Gemini and conventional cationic surfactants, *Nonferrous Metals Society of China* 19 (2009) 446-453.

- [25] O.H. Han, M.K. Kim, B.G. Kim, N. Subasinghe, C.H. Park, Fine coal beneficiation by column flotation, *Fuel Processing Technology* 126 (2014) 49-59.
- [26] J. Choi, E. Lee, S.Q. Choi, S. Lee, Y. Han, H. Kim, Arsenic removal from contaminated soils for recycling via oil agglomerate flotation, *Chemical Engineering Journal* 285 (2016) 207–217.
- [27] J. Clifton, P. McDonald, A. Plater, F. Oldfield, An investigation into the efficiency of particle size separation using Stokes' law, *Earth Surface Processes and Landforms* 24 (1999) 725-730.
- [28] B.W. Flemming, A revised textural classification of gravel-free muddy sediments on the basis of ternary diagrams, *Continental Shelf Research* 20 (2000) 1125-1137.
- [29] J.C.M. Chapelain, S. Faure, D. Beneventi, Clay Flotation: Effect of TTAB Cationic Surfactant on Foaming and Stability of Illite Clay Microaggregates Foams, *Industrial and Engineering Chemistry Research* 55 (2016) 2191–2201.
- [30] S.J. Neethling, J.J. Cilliers, The entrainment factor in froth flotation: Model for particle size and other operating parameter effects, *International Journal of Mineral Processing* 93 (2009) 141–148.
- [31] L. Wang, Y. Peng, K. Runge, D. Bradshaw, A review of entrainment: Mechanisms, contributing factors and modelling in flotation, *Minerals Engineering* 70 (2015) 77–91.
- [32] X. Zheng, J.P. Franzidis, N.W. Johnson, E.V. Manlapig, Modelling of entrainment in industrial flotation cells: the effect of solids suspension, *Minerals Engineering* 18 (2005) 51-58.
- [33] B. Haffner, Y. Khidas, O. Pitois, The drainage of foamy granular suspensions, *Journal of Colloid and Interface Science* 458 (2015) 200-208.

- [34] R.M. Guillermic, A. Salonen, J. Emile, A. Saint-Jalmes, Surfactant foams doped with laponite: unusual behaviors induced by aging and confinement, *Soft Matter* 5 (2009) 4975-4982.
- [35] R.M. Rahman, S. Ata, G.J. Jameson, The effect of flotation variables on the recovery of different particle size fractions in the froth and the pulp, *International Journal of Mineral Processing* 106-109 (2012) 70–77.
- [36] M. Falutsu, G.S. Dobby, Direct measurement of froth drop back and collection zone recovery in a laboratory flotation column, *Minerals Engineering* 2 (1989) 377–386.
- [37] S.M. Feteris, J.A. Frew, A. Jowett, Modelling the effect of froth depth in flotation, *International Journal of Mineral Processing* 20 (1987) 121–135.
- [38] X. Luo, B. Feng, C. Wong, J. Miao, B. Ma, H. Zhou, The critical importance of pulp concentration on the flotation of galena from a low grade lead–zinc ore, *Journal of Materials Research and Technology* 5 (2016) 131-135.
- [39] B. K. Gorain, J. P. Franzidis, E.V. Manlapig, Studies on impeller type, impeller speed and air flow rate in an industrial scale flotation cell. Part 4: Effect of bubble surface area flux on flotation performance, *Minerals Engineering* 10 (1997) 367-379.
- [40] D. Beneventi, X. Rousset, E. Zeno, Modelling transport phenomena in a flotation deinking column: Focus on gas flow, pulp and froth retention time, *International Journal of Mineral Processing* 80 (2006) 43-57.
- [41] A. R. Laplante, J. M. Toguri, H. W. Smith, The effect of air flow rate on the kinetics of flotation. Part 1: The transfer of material from the slurry to the froth, *International Journal of Mineral Processing* 11 (1983) 203-219.

Supplementary material

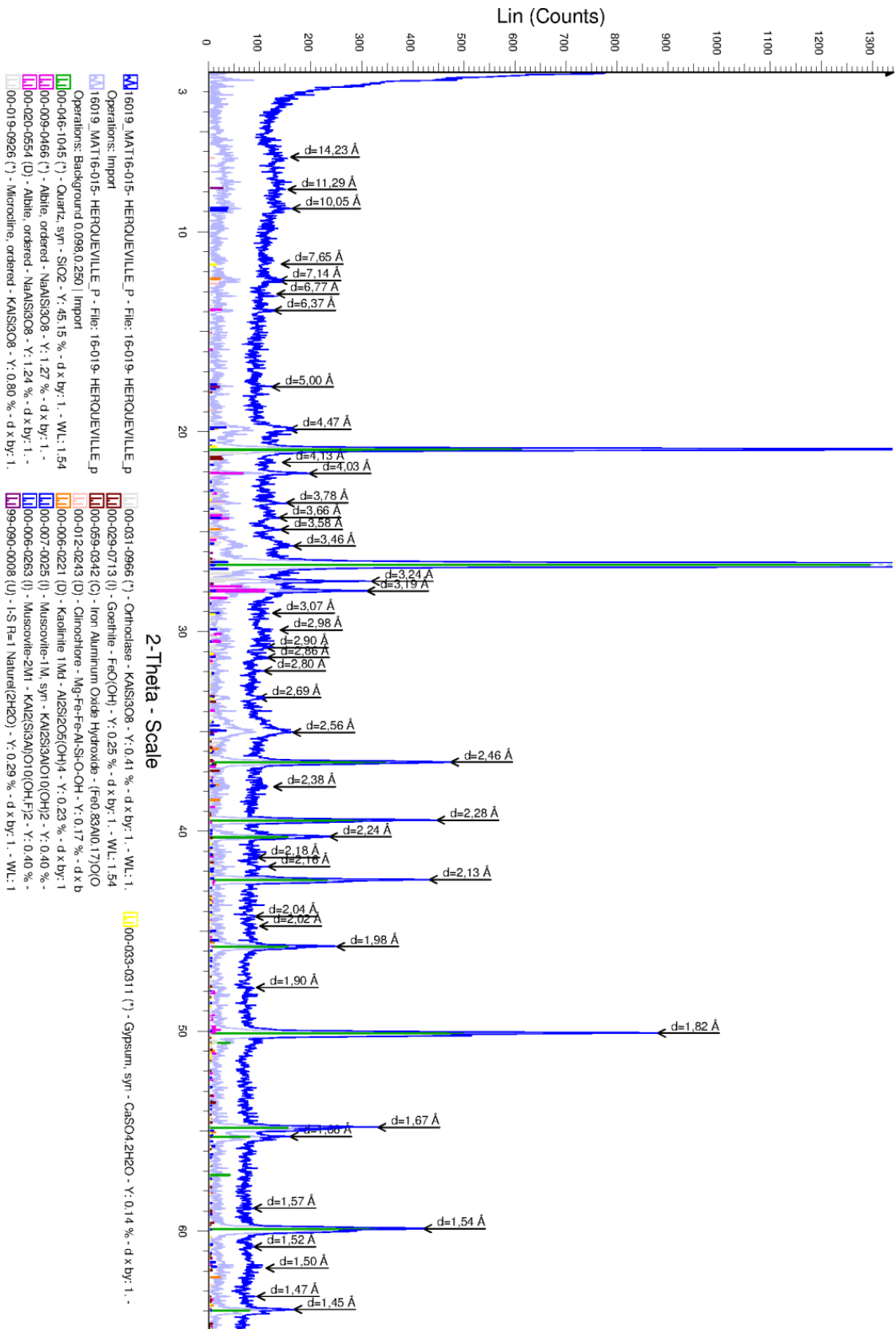


Fig. A. X-Ray Diffractogram of the raw soil.

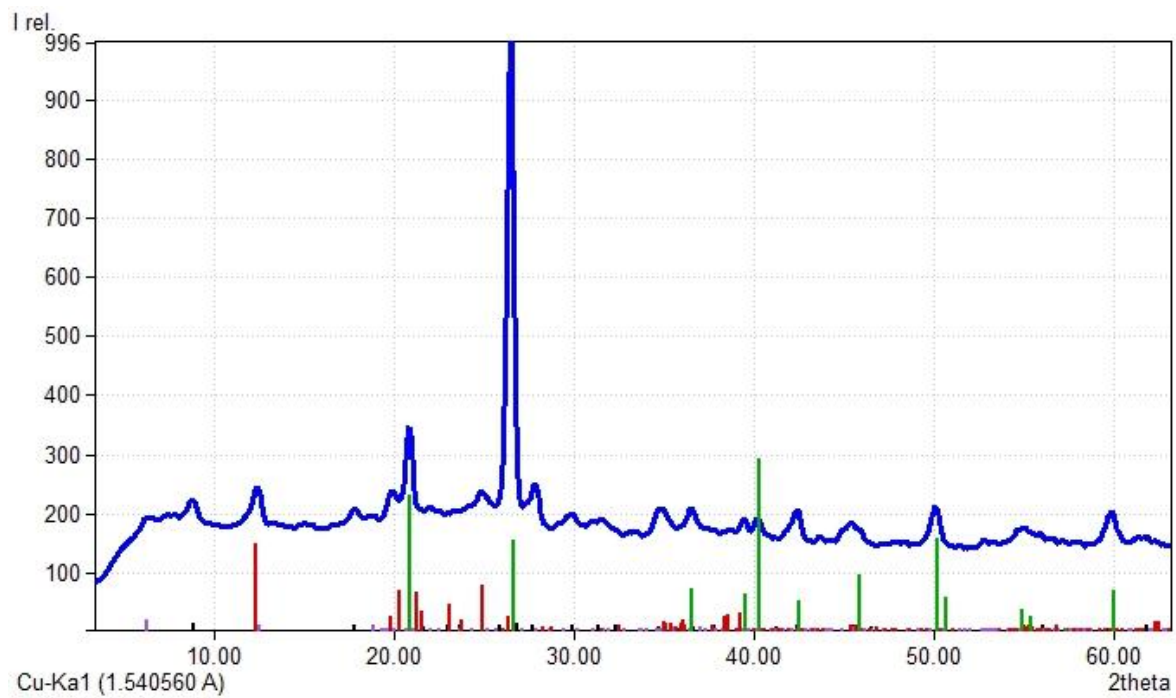


Fig. B. X-Ray Diffractogram of the 2-20 μm froth particles separated from soil. Standards: quartz (green lines), illite (black lines), chlorite (violet lines), kaolinite (red lines).